Electronic Supplementary Material (ESI) for Chemical Communications.

Supporting Information

Rare-earth-metal half-sandwich complexes incorporating methyl, methylidene, and hydrido ligands

Dennis A. Buschmann,[a] Lion Schumacher[a] and Reiner Anwander*[a]

[a] Eberhard Karls Universität Tübingen, Institut für Anorganische Chemie, Auf der Morgenstelle 18, 72076 Tübingen, Germany

Correspondence: reiner.anwander@uni-tuebingen.de

Table of Contents

Experimental Procedures

General considerations.

All manipulations were performed under rigorous exclusion of air and moisture using standard Schlenk and glovebox techniques (MBraun MB200B; <0.1 ppm O_2, <0.1 ppm H_2O, argon atmosphere). The solvents *n*-hexane, toluene, THF and Et_2O were purified using Grubbs-type columns (MBraun SPS, solvent purification system). [D_8]THF (99.5%, Sigma-Aldrich) was dried over Na/K-alloy for 24 h, vacuum transferred prior to use and stored inside a glovebox. [D_4]methanol (≥ 99.8%, Sigma-Aldrich) was stored over molecular sieve inside a glovebox. Benzophenone (99%, Fluka) was used without further purification. Cyclohexanone (>99%, Acros Organics) was destilled prior to use. 9-fluorenone (98%, Sigma-Aldrich) was sublimed prior to use. 1,2,3,4,5-pentamethyl cyclopentadiene (HCp*) (98%, abcr) was used as received. Homoleptic $Ln(AlMe_4)_3$ (Ln = Y, Dy),[1] half-sandwich complexes $Cp^*Ln(AlMe_4)_2$ (Ln = Y, Dy)[2,3] and trinuclear complex $[Cp^*_3Y_3(\mu_2\text{-}CH_3)_3(\mu_3\text{-}CH_3)(\mu_3\text{-}CH_2)(thf)_2]$ (**I**)[4] were synthesized according to literature procedures. NMR spectra of air and moisture sensitive compounds were recorded by using J. Young valve NMR tubes on a Bruker AVII+400 spectrometer (^{1}H: 400.11 MHz; ^{13}C: 100.61 MHz) and on a Bruker AVII+500 spectrometer (^{1}H: 500.13 MHz, ^{13}C: 125.76 MHz). NMR chemical shifts are referenced to internal solvent resonances and reported in parts per million relative to tetramethyl silane. Coupling constants are given in Hertz. Elemental analyses were performed on an Elementar Vario Micro Cube. IR spectra were recorded on a NICOLET 6700 FTIR spectrometer with a DRIFT cell (KBr window, Kubelka-Munk conversion).

$[Cp^*_3Y_3(\mu_2\text{-}CH_3)(\mu_3\text{-}CH_2)(\mu_3\text{-}H)(thf)_3]$ (1^Y). $Cp^*Y(AlMe_4)_2$ (49.7 mg, 0.125 mmol) was dissolved in *n*-hexane (2 mL) and diethyl ether (37.1 mg, 0.5 mmol) was added, which led to immediate precipitation of amorphous $[Cp^*YMe_2]_3$. After stirring the suspension for 30 min at ambient temperature, the product was separated by centrifugation. The precipitate was washed with *n*-hexane (3 x 2 mL) and then $[Cp^*YMe_2]_3$ was dried under vacuum (yield: 23.4 mg, 0.092 mmol, 74%) for 30 min. Afterwards, $[Cp^*YMe_2]_3$ was dissolved in THF (1 mL), the formation of gas (CH_4) could be observed, and the solution was stored at ambient temperature. Over a period of five days, a color was observed (colorless, yellow (1 d), orange (3 d), red (5 d)). After five days, light yellow crystals formed. The red supernatant was removed, and the crystalline product was washed with *n*-hexane (3 x 2 mL) and with *n*-pentane (1 x 2 mL). The crystalline product was dried under vacuum (yield: 7.5 mg, 7.9 μmol, 26%). The overall yield was increased to 76% (22.1 mg, 0.023 mmol) by treating the red supernatant with the same workup procedure as described before. ^{1}H NMR (400 MHz, [D_8]THF, 26 °C): δ = 4.61 (q, $^1J_{YH}$ = 12.2 Hz, 1H, μ_3-*H*), 3.61 (m, coord. C_4H_8O), 1.90 (s, 45H, $CpCH_3$), 1.77 (m, coord. C_4H_8O), -0.28 (q, $^2J_{YH}$ = 3.8 Hz, 2H, μ_3-CH_2), -1.03 (s, 9H, μ_2-CH_3) ppm. $^{13}C\{^1H\}$ NMR (126 MHz, [D_8]THF, 26 °C): δ = 115.0 (C_5Me_5), 95.3 (μ_3-CH_2, HSQC), 21.3 (μ_2-CH_3, $^1J_{YC}$ = 22.8 Hz), 12.2 ($Cp(CH_3)_5$) ppm. IR(DRIFT): $\tilde{\nu}$ = 2958 (m), 2901 (m), 2857 (m), 2715 (vw), 1445 (w), 1373 (vw), 1342 (vw), 1294 (vw), 1249 (vw), 1154 (w), 1034 (s), 955 (s), 923 (m), 878 (vs), 665 (w), 593 (m), 559 (m), 540 (m), 515 (vs), 502 (vs), 492 (s), 478 (s), 455 (s), 444 (s), 432 (m), 425 (s), 413 (vs) cm^{-1}. Elemental analysis of $\mathbf{1^Y}$ calculated for $C_{46}H_{81}Y_3O_3$ (948.87 g/mol): C 58.23%, H 8.60%; found: C 57.10%, H 8.33%. The low carbon value can be attributed to a loss of coordinated THF upon drying the product under vacuum.

[Cp*$_3$Dy$_3$(μ_2-Me)(μ_3-CH$_2$)(μ_3-H)(thf)$_3$] ($\mathbf{1^{Dy}}$). Cp*Dy(AlMe$_4$)$_2$ (118.0 mg, 0.25 mmol) was dissolved in *n*-hexane (2 mL) and diethyl ether (74.1 mg, 1.0 mmol) was added, which lead to immediate precipitation of amorphous [Cp*DyMe$_2$]$_3$. After stirring the suspension for 30 min at ambient temperature, the product was separated by centrifugation. The precipitate was washed with *n*-hexane (3 x 2 mL) and then [Cp*DyMe$_2$]$_3$ was dried under vacuum (yield: 65.1 mg, 0.2 mmol, 79%) for 30 min. Afterwards, 10 mg (0.03 mmol) of [Cp*DyMe$_2$]$_3$ were dissolved in THF (0.5 mL), the formation of gas (CH$_4$) was observed, and the solution was stored at ambient temperature. Over a period of five days, a color change was observed (colorless, yellow (1 d), orange (3 d)). After eight days, the solution was stored at -40 °C, followed by partial removal of the solvent under vacuum until colorless crystals formed. The orange supernatant was removed, and the crystalline product was washed with *n*-hexane (3 x 2 mL) and with *n*-pentane (1 x 2 mL). The crystalline product was dried under vacuum (yield: 2.5 mg, 2.1 μmol, 21%). The overall yield was increased to 74% (9.0 mg, 7.7 µmol) by treating the orange supernatant with the same workup procedure as described before. IR(DRIFT): $\tilde{\nu}$ = 2961 (s), 2910 (vs), 2901 (vs), 2856 (vs), 2721 (vw), 1487 (vw), 1436 (m), 1375 (w), 1340 (vw), 1299 (vw), 1244 (vw), 1179 (w), 1086 (w), 1057 (w), 1020 (s), 912 (m), 868 (s), 800 (w), 740 (w), 671 (s), 619 (m), 598 (m), 587 (m), 565 (m), 549 (m), 539 (m), 529 (m), 515 (m), 502 (s), 488 (m), 469 (m), 457 (m), 451 (m), 445 (m), 434 (s), 427 (s), 419 (s) cm^{-1}. Elemental analysis of $\mathbf{1^{Dy}}$ calculated for C$_{46}$H$_{81}$Dy$_3$O$_3$ (1169.65 g/mol): C 47.24%, H 6.98%; found: C 47.46%, H 6.35%.

Reaction of Cp*$_3$Y$_3$(μ_2-CH$_3$)$_3$(μ_3-CH$_3$)(μ_3-CH$_2$)(thf)$_2$ (I) with THF. Compound **I** was synthesized according to literature procedures.[4] Afterwards, **I** was redissolved in THF and stirred at ambient temperature. Samples were repeatedly taken from the reaction mixture, the solvent was removed completely under vacuum, the residual solid was redissolved in [D$_8$]THF, and a ^{1}H NMR spectrum was recorded to monitor the reaction progress.

General procedure for methylidene transfer reactions. All reactions were monitored via ^{1}H NMR spectroscopy. In a *J. Young* valve NMR tube, 5 mg of $\mathbf{1^{Y}}$ were dissolved in [D$_8$]THF (0.3 mL). Two equivalents of the respective ketone (benzophenone, cyclohexanone, 9-fluorenone) or an equimolar amount of 9-fluorenone were dissolved in [D$_8$]THF (0.2 mL) and added, and the tube was sealed immediately. After 15 minutes, during which the tube was shaken repeatedly, a ^{1}H NMR spectrum was recorded. The yields of all reactions were calculated from the integral ratio olefinic functionality/Y-CH$_2$.

Reaction with [D$_4$]methanol. In a *J. Young* NMR-tube, complex $\mathbf{1^{Y}}$ (5 mg, 0.005 mmol) was dissolved in [D$_8$]THF, [D$_4$]methanol was added (0.05 mL), and the tube was sealed immediately. Gas evolution was observed for approximately 3 min. After 5 min, a ^{1}H NMR spectrum was recorded.

NMR Spectroscopy

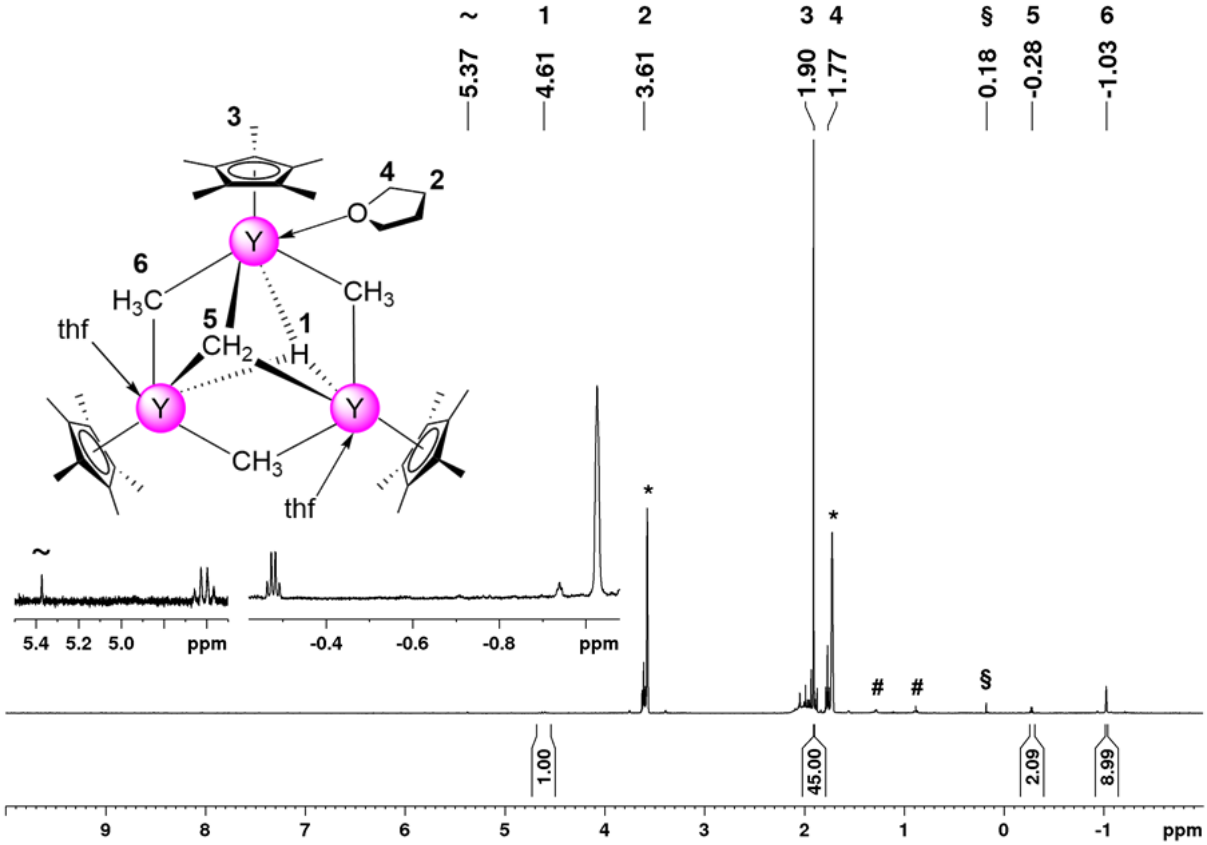

Figure S2. ^{1}H NMR spectrum (400 MHz) of **1^{Y}** in [D$_8$]THF at 26 °C. The solvent residual signals are marked with an asterisk (#: *n*-hexane, §: methane, ~: ethene).

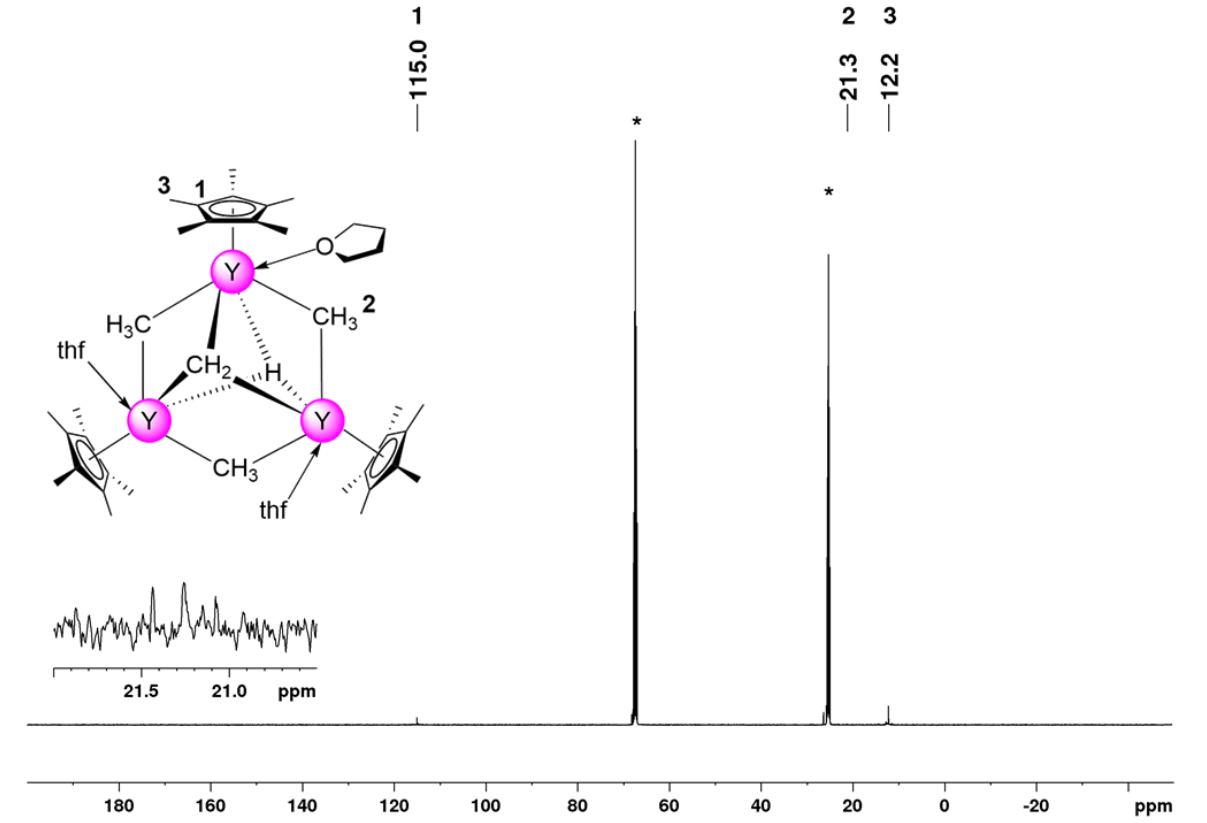

Figure S1. ^{13}C{^{1}H} NMR spectrum (126 MHz) of **1^{Y}** in [D$_8$]THF at 26 °C. The solvent residual signals are marked with an asterisk.

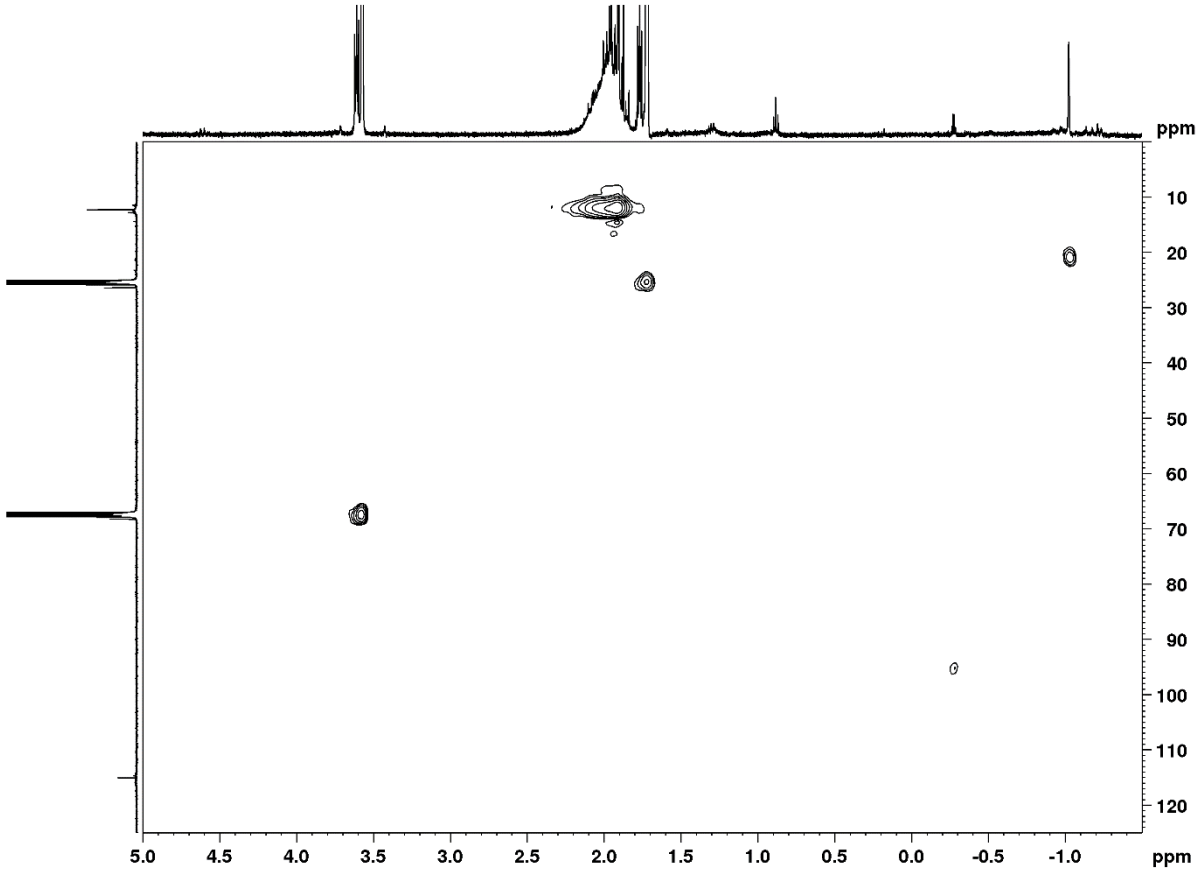

Figure S3. HSQC NMR spectrum of $\mathbf{1^Y}$ in [D_8]THF at 26 °C.

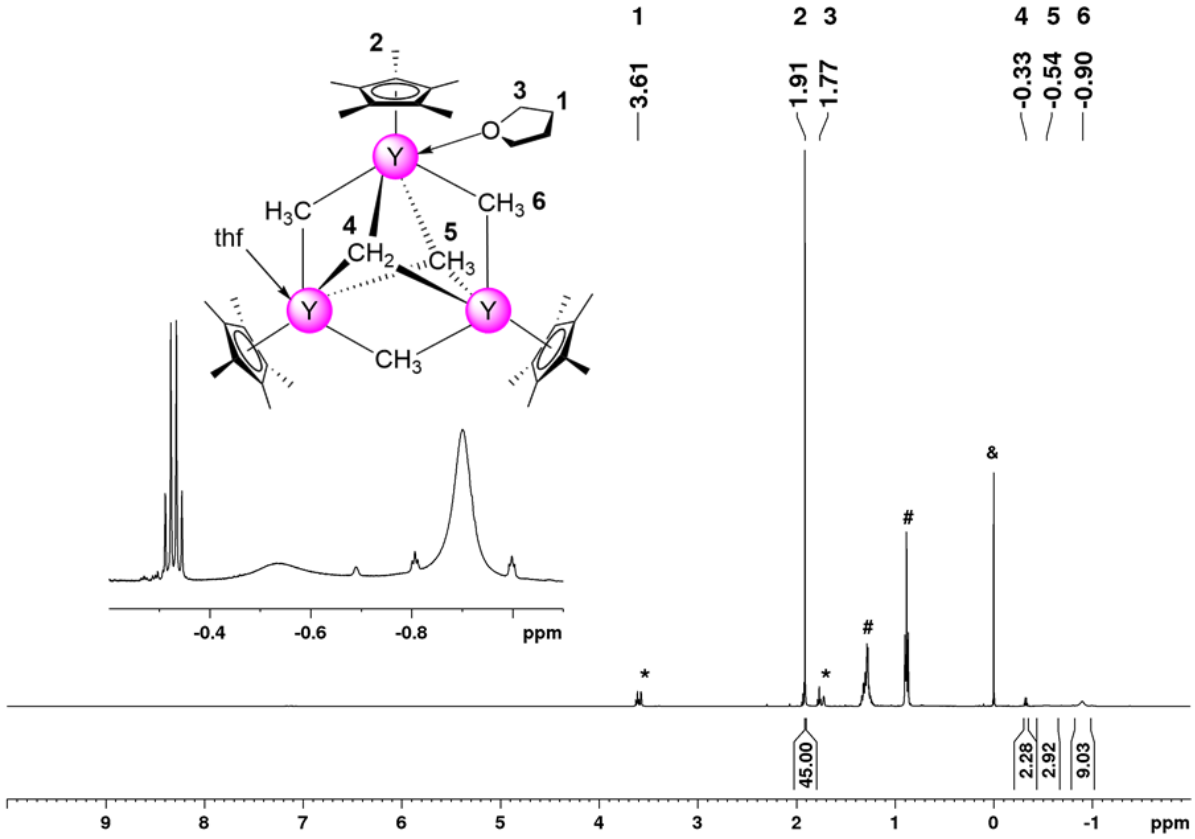

Figure S4. ^{1}H NMR spectrum (400 MHz) of [Cp*$_3$Y$_3$(μ_2-CH$_3$)$_3$(μ_3-CH$_3$)(μ_3-CH$_2$)(thf)$_2$] (**I**) in [D$_8$]THF at 26 °C. The solvent residual signals are marked with an asterisk (#: *n*-hexane, &: SiMe$_4$).

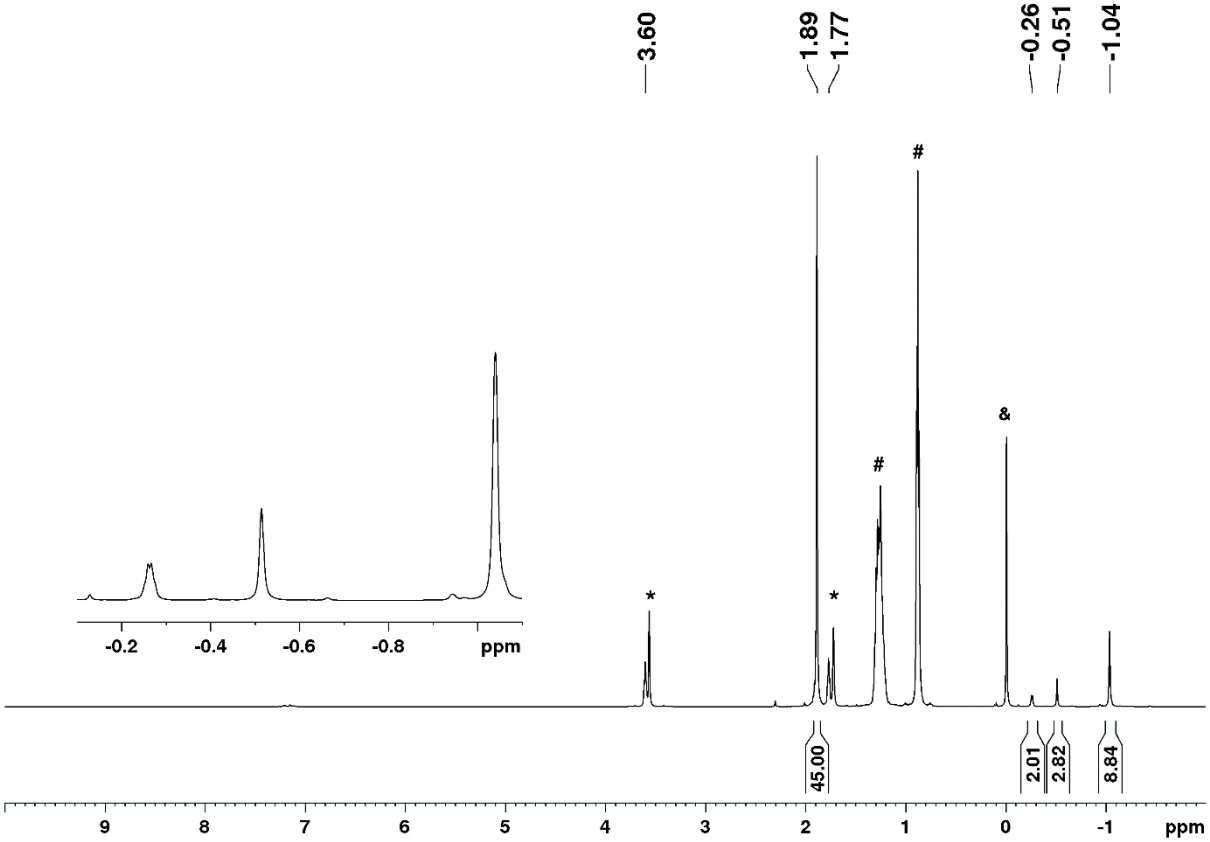

Figure S5. ^{1}H NMR spectrum (500 MHz) of [Cp*$_3$Y$_3$(μ_2-CH$_3$)$_3$(μ_3-CH$_3$)(μ_3-CH$_2$)(thf)$_2$] (**I**) in [D$_8$]THF at -60 °C. The solvent residual signals are marked with an asterisk (#: *n*-hexane, &: SiMe$_4$).

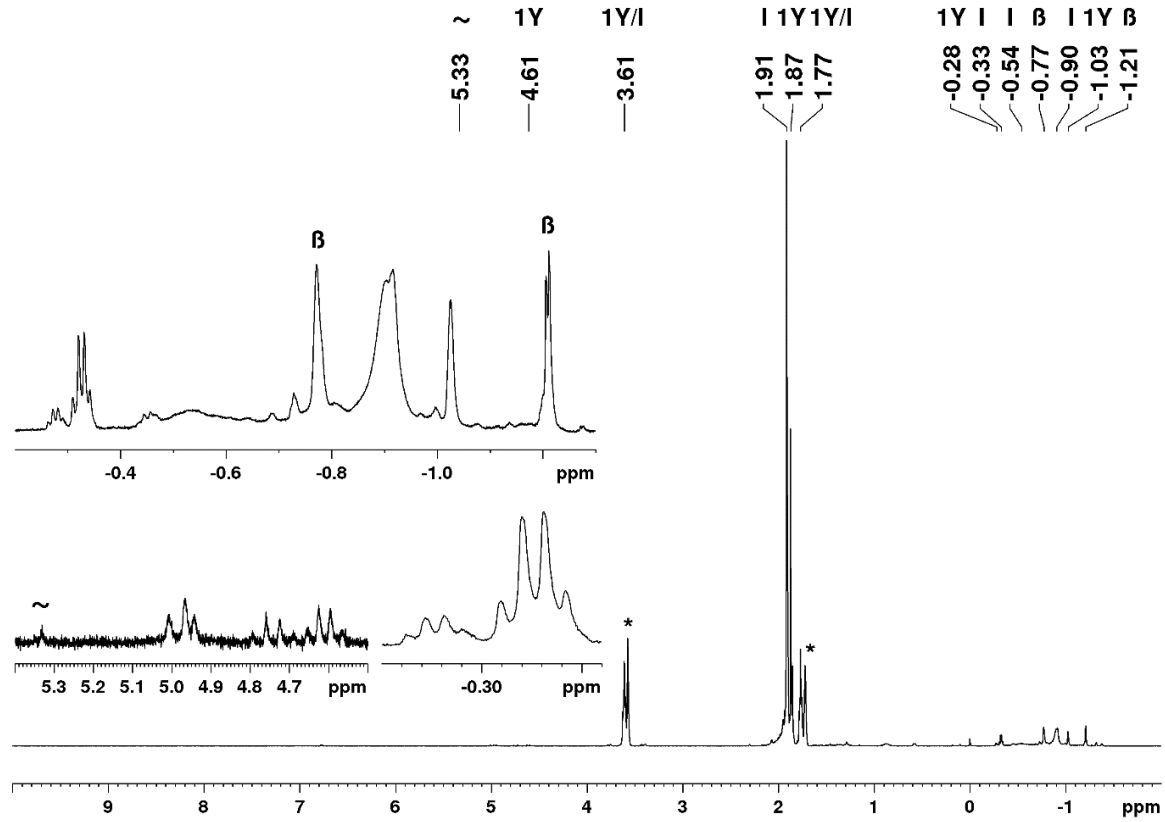

Figure S6. ^{1}H NMR spectrum (400 MHz) of [Cp*$_3$Y$_3$(μ_2-CH$_3$)$_3$(μ_3-CH$_3$)(μ_3-CH$_2$)(thf)$_2$] (**I**) in [D$_8$]THF at 26 °C after 7 days. The solvent residual signals are marked with an asterisk (~: ethene, ß: unknown yttrium species).

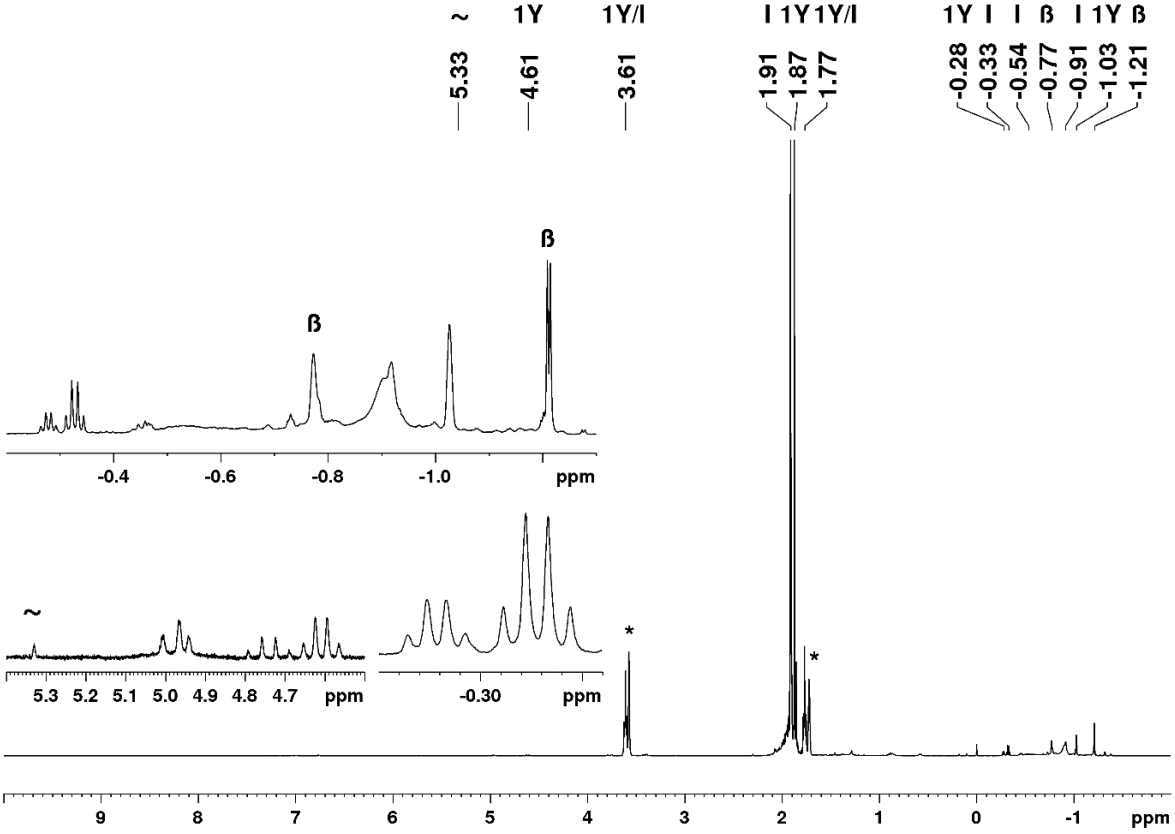

Figure S7. ^{1}H NMR spectrum (400 MHz) of [Cp*$_3$Y$_3$(μ_2-CH$_3$)$_3$(μ_3-CH$_3$)(μ_3-CH$_2$)(thf)$_2$] (**I**) in [D$_8$]THF at 26 °C after 14 days. The solvent residual signals are marked with an asterisk (~: ethene, ß: unknown yttrium species).

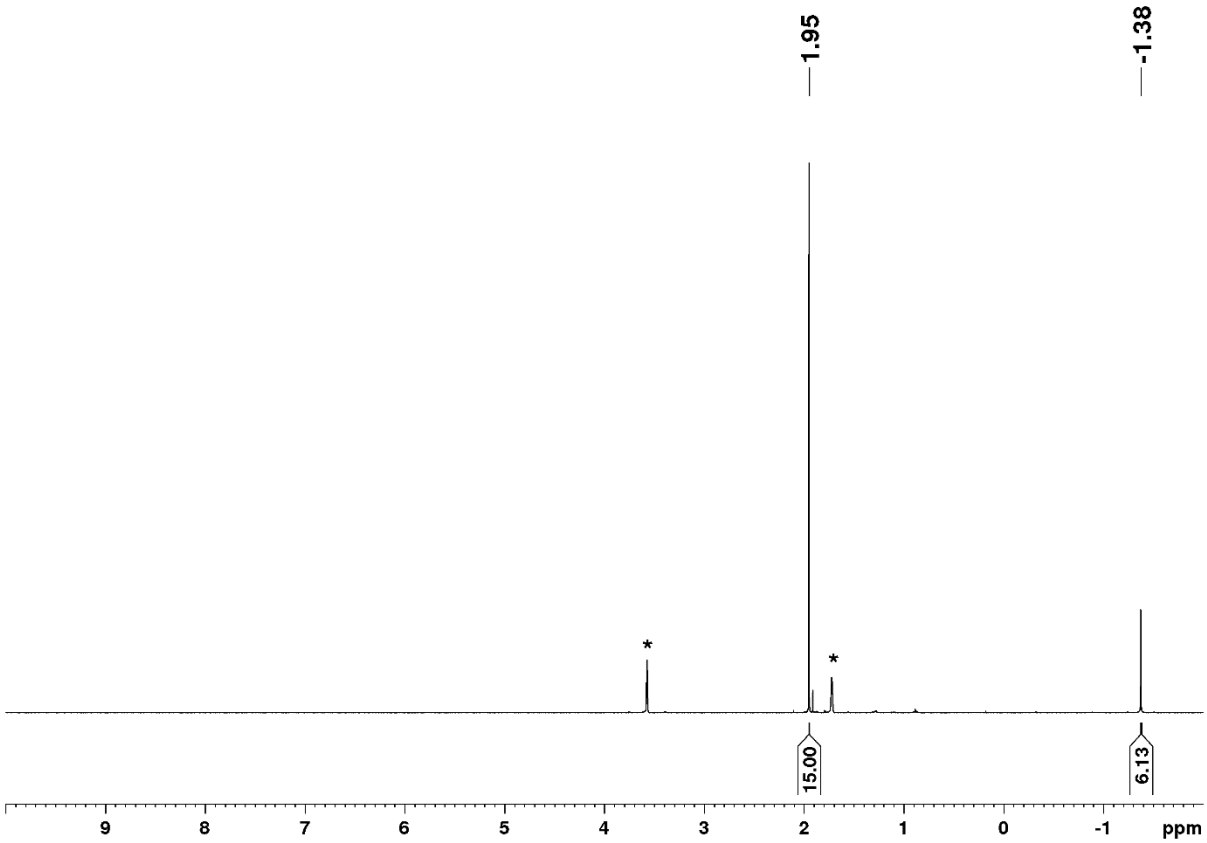

Figure S8. ^{1}H NMR spectrum (400 MHz) of $[Cp^*YMe_2]_3$ in $[D_8]$THF at 26 °C immediately after the addition of $[D_8]$THF. The solvent residual signals are marked with an asterisk.

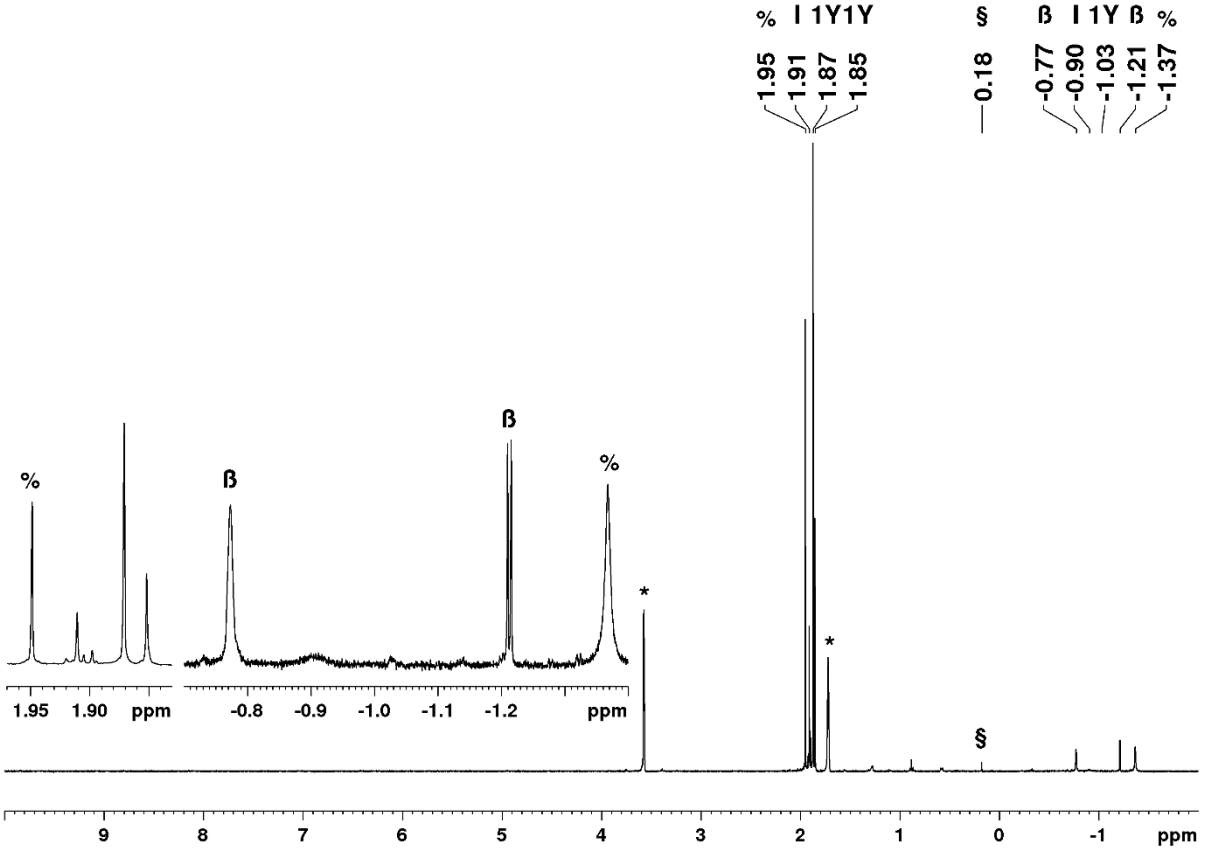

Figure S9. ^{1}H NMR spectrum (400 MHz) of $[Cp^*YMe_2]_3$ in $[D_8]$THF at 26 °C after two days. The solvent residual signals are marked with an asterisk (%: $[Cp^*YMe_2]_3$, §: methane, ß: unknown yttrium species).

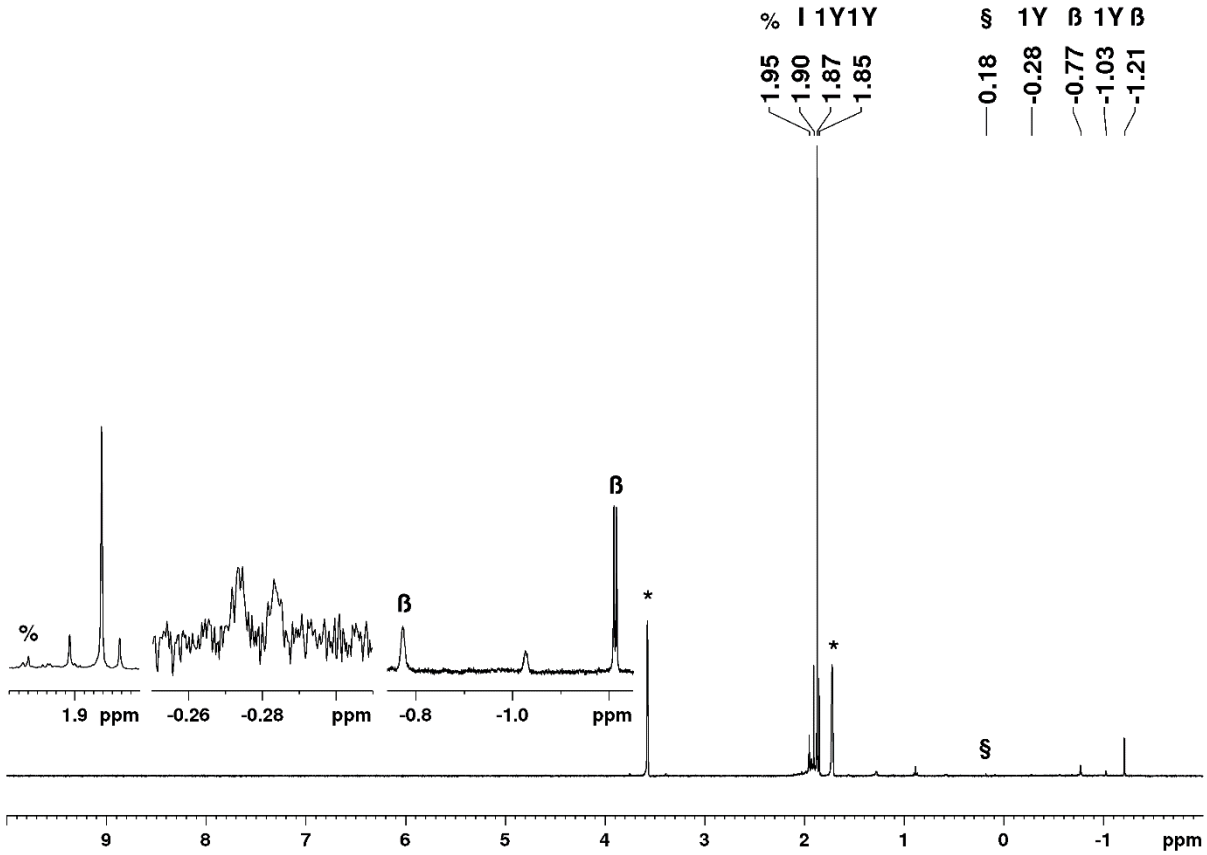

Figure S10. ^{1}H NMR spectrum (400 MHz) of $[Cp^{*}YMe_2]_3$ in $[D_8]$THF at 26 °C after 10 days. The solvent residual signals are marked with an asterisk (%: $[Cp^{*}YMe_2]_3$, §: methane, ß: unknown yttrium species).

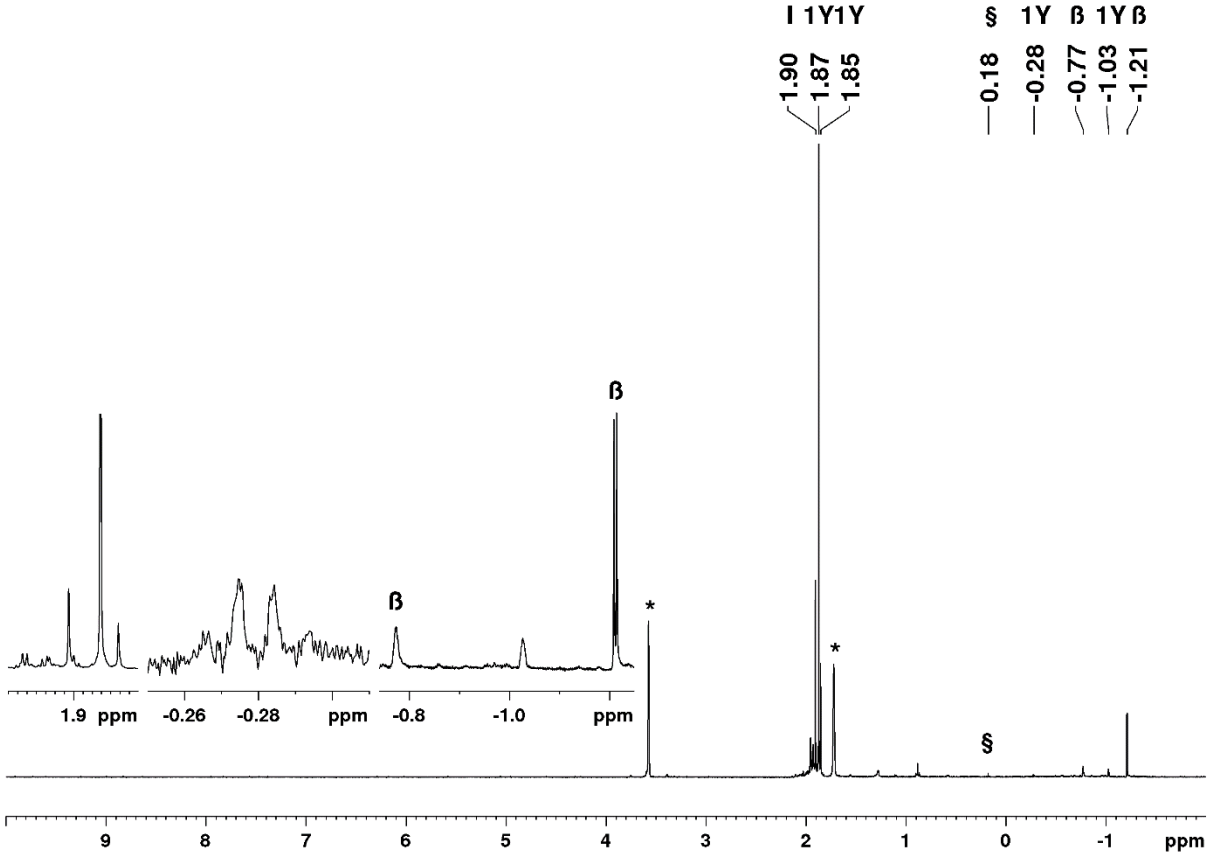

Figure S11. ^{1}H NMR spectrum (400 MHz) of $[Cp^{*}YMe_2]_3$ in $[D_8]$THF at 26 °C after 14 days. The solvent residual signals are marked with an asterisk (§: methane, ß: unknown yttrium species).

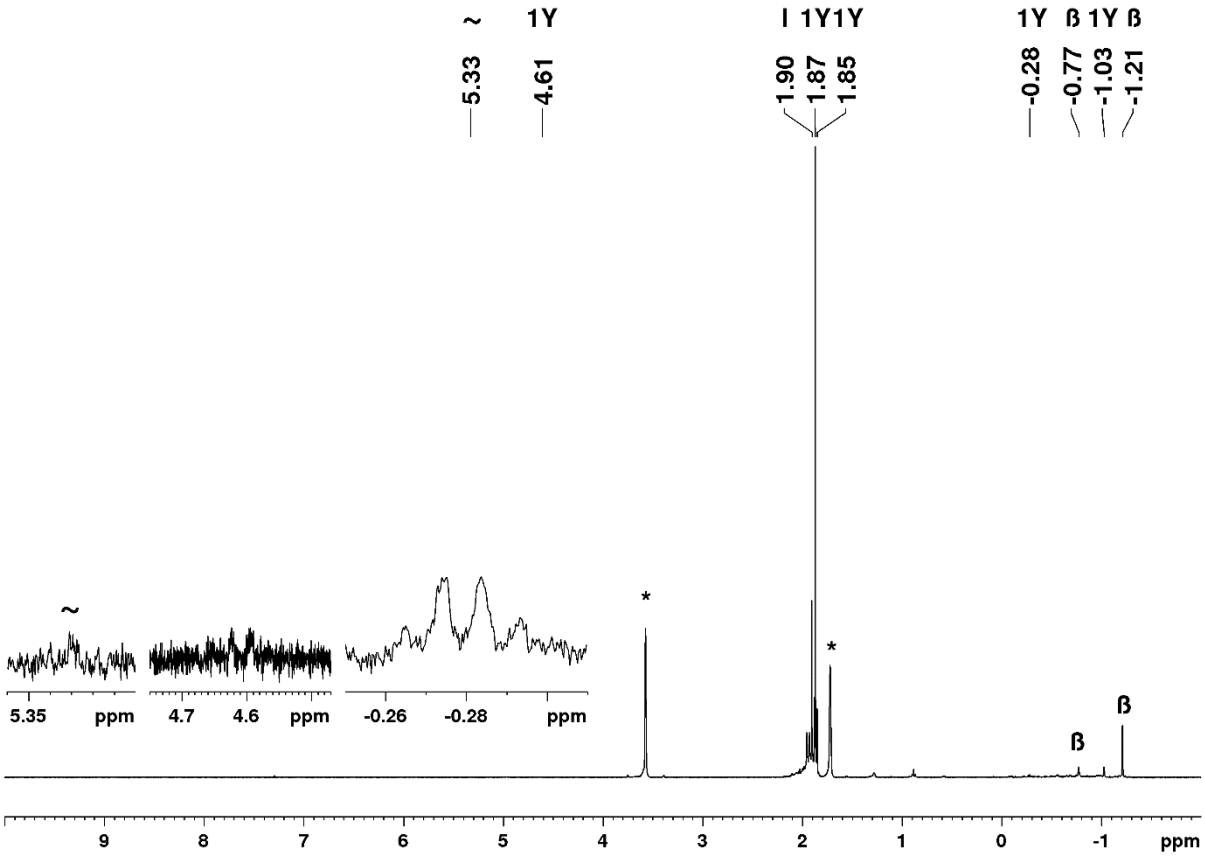

Figure S12. ^{1}H NMR spectrum (400 MHz) of $[Cp^{*}YMe_2]_3$ in $[D_8]$THF at 26 °C after 17 days. The solvent residual signals are marked with an asterisk (~: ethene, ß: unknown yttrium species).

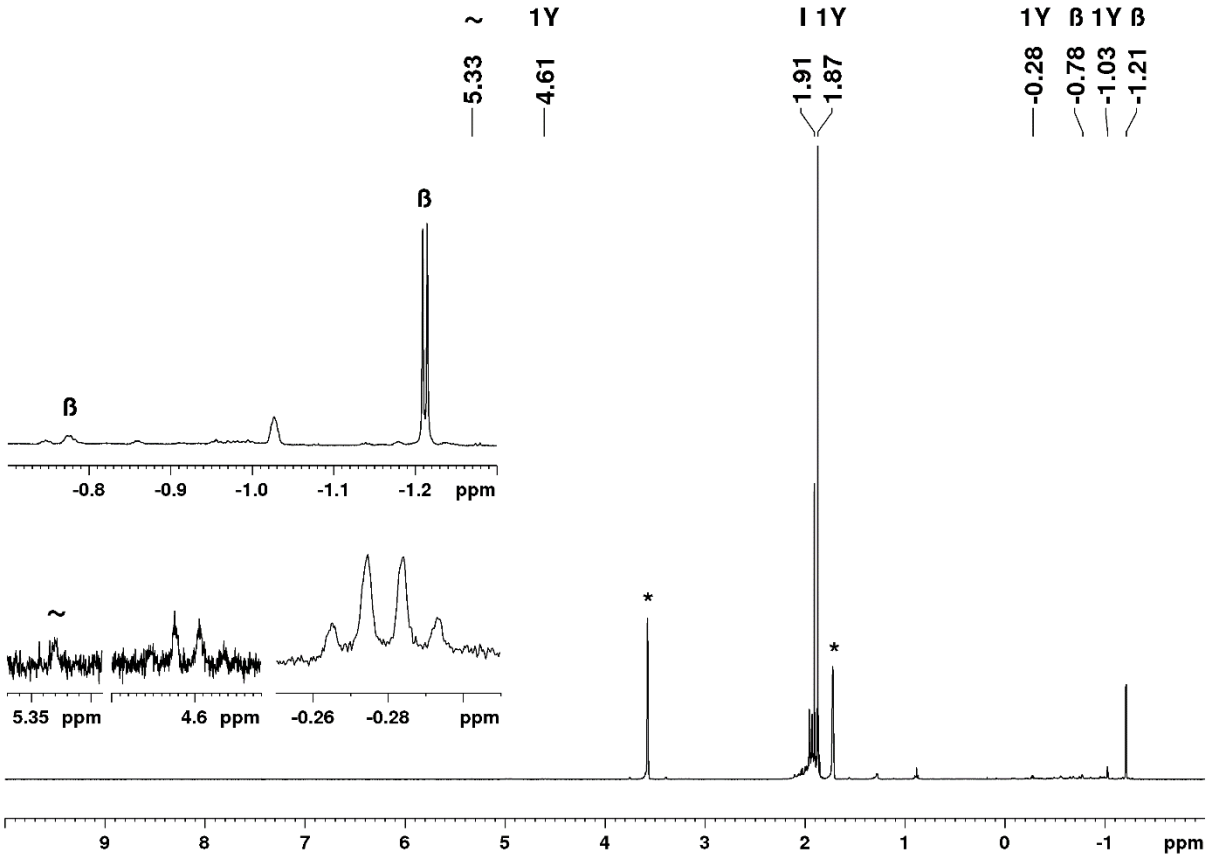

Figure S13. ^{1}H NMR spectrum (400 MHz) of $[Cp^{*}YMe_2]_3$ in $[D_8]$THF at 26 °C after 24 days. The solvent residual signals are marked with an asterisk (~: ethene, ß: unknown yttrium species).

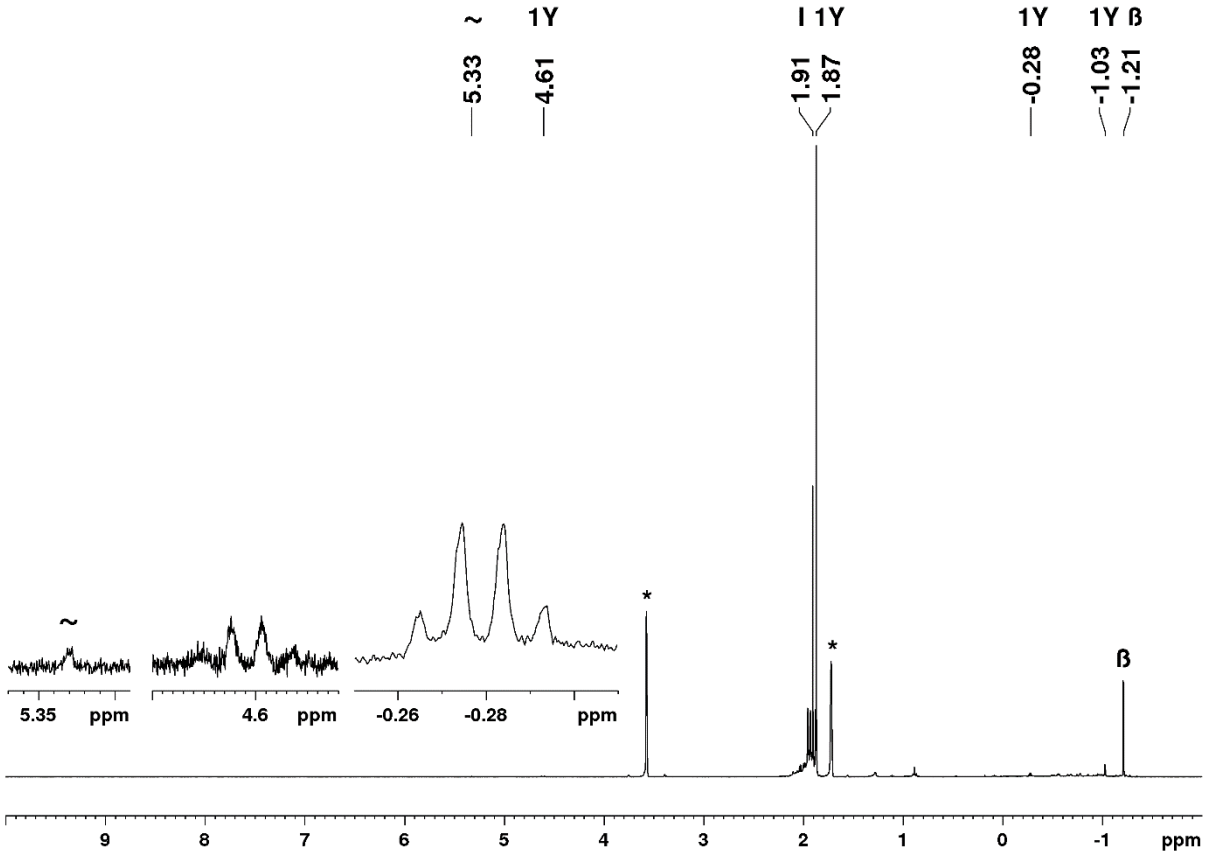

Figure S14. ^{1}H NMR spectrum (400 MHz) of $[Cp^*YMe_2]_3$ in $[D_8]$THF at 26 °C after 30 days. The solvent residual signals are marked with an asterisk (~: ethene, ß: unknown yttrium species).

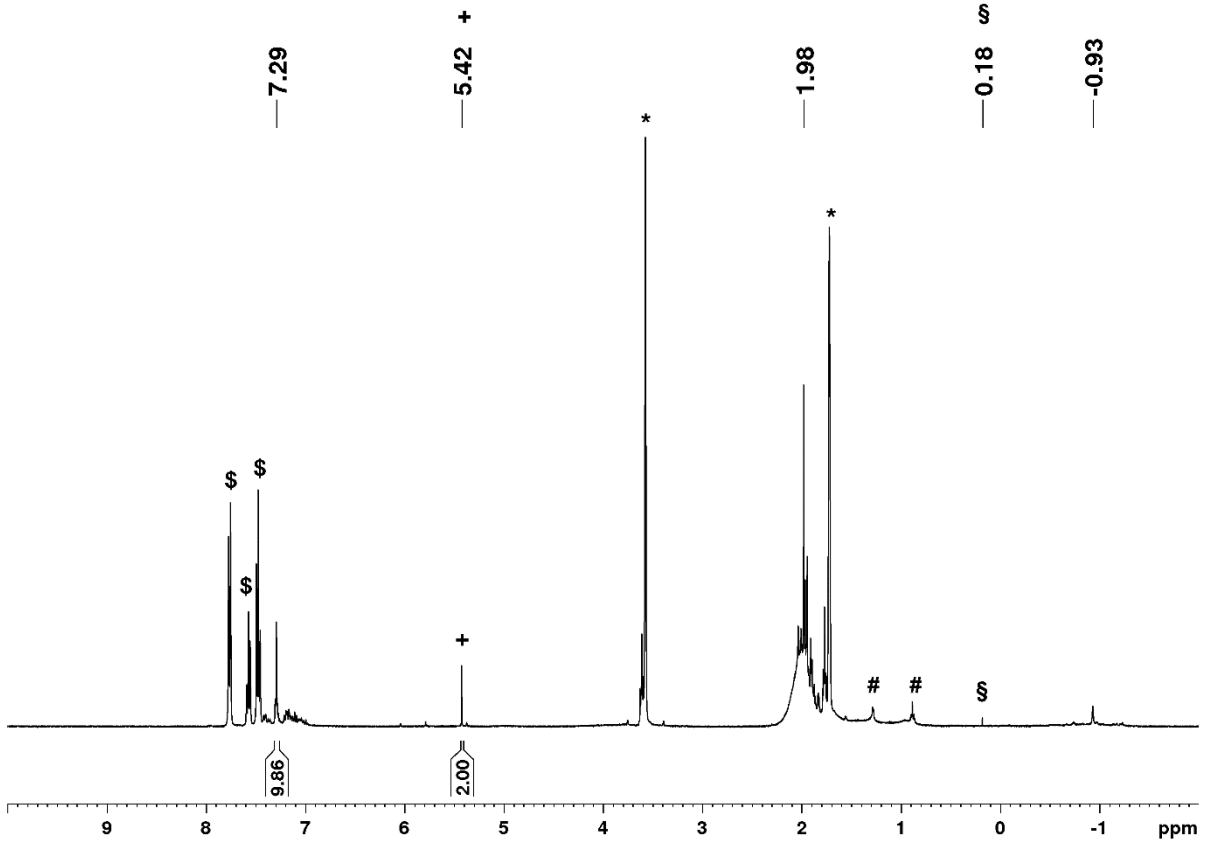

Figure S15. ^{1}H NMR spectrum (400 MHz) of $\mathbf{1^Y}$ in $[D_8]$THF at 26 °C, 15 minutes after addition of benzophenone. The solvent residual signals are marked with an asterisk (+: methylene, #: *n*-hexane, §: methane, $: benzophenone).

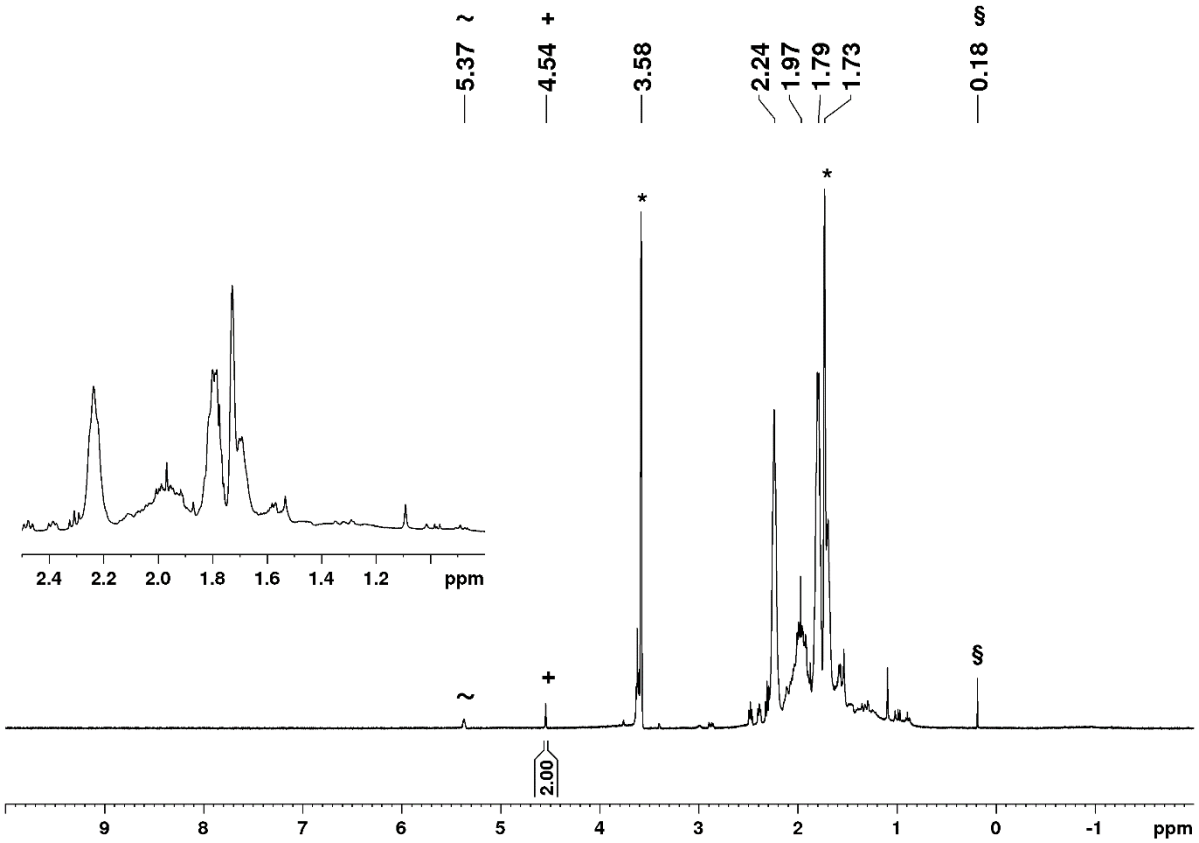

Figure S16. ^{1}H NMR spectrum (400 MHz) of $\mathbf{1}^{\mathbf{Y}}$ in [D_8]THF at 26 °C, 15 minutes after addition of cyclohexanone. The solvent residual signals are marked with an asterisk (+: methylene, §: methane, ~: ethene).

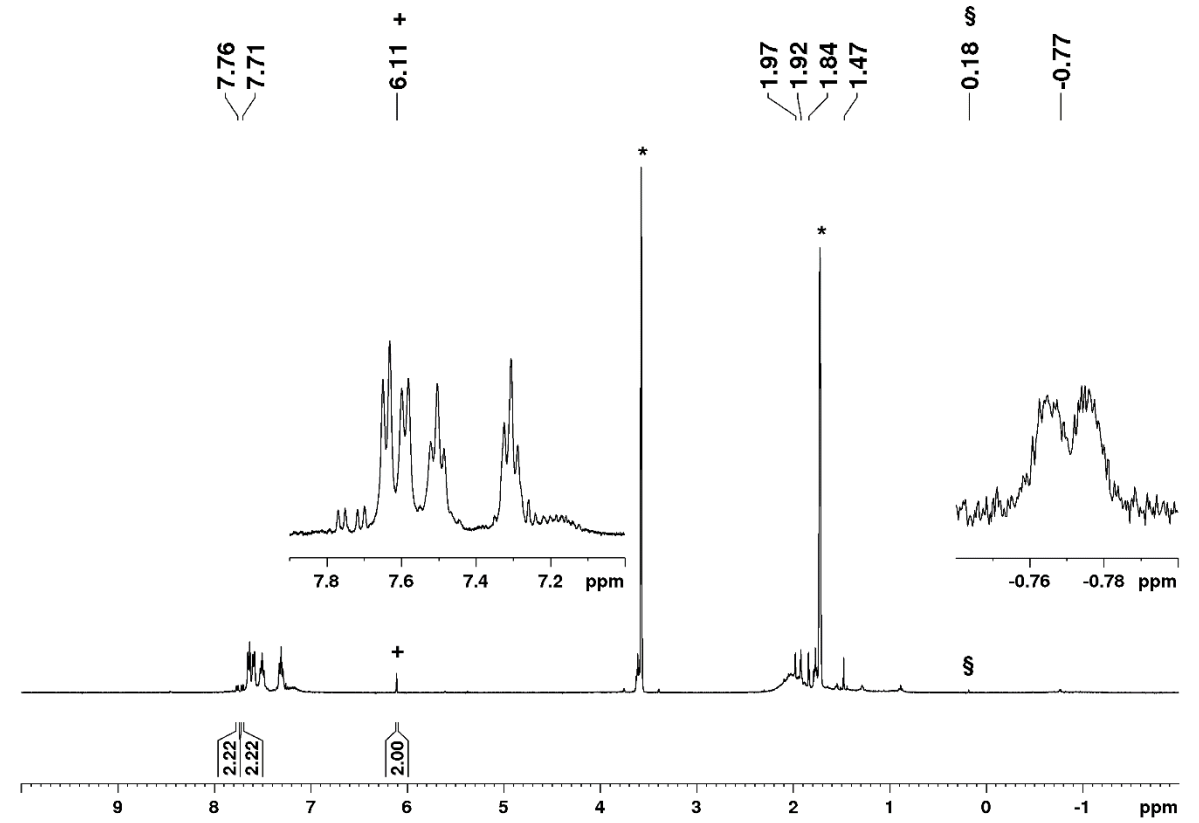

Figure S17. ^{1}H NMR spectrum (400 MHz) of $\mathbf{1}^{\mathbf{Y}}$ in [D_8]THF at 26 °C, 15 minutes after addition of 9-fluorenone. The solvent residual signals are marked with an asterisk (+: methylene, §: methane).

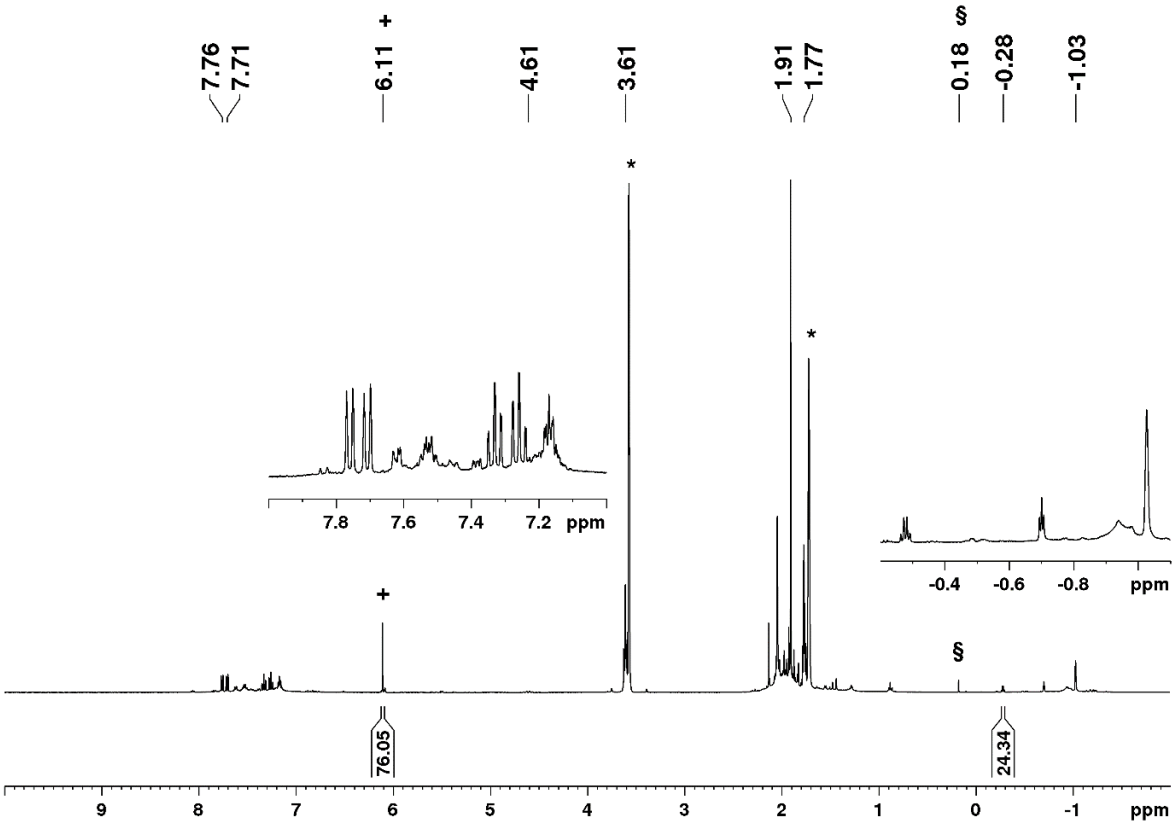

Figure S18. ^{1}H NMR spectrum (400 MHz) of $\mathbf{1}^{Y}$ in [D_8]THF at 26 °C, 15 minutes after addition of an equimolar amount of 9-fluorenone. The solvent residual signals are marked with an asterisk (+: methylene, §: methane).

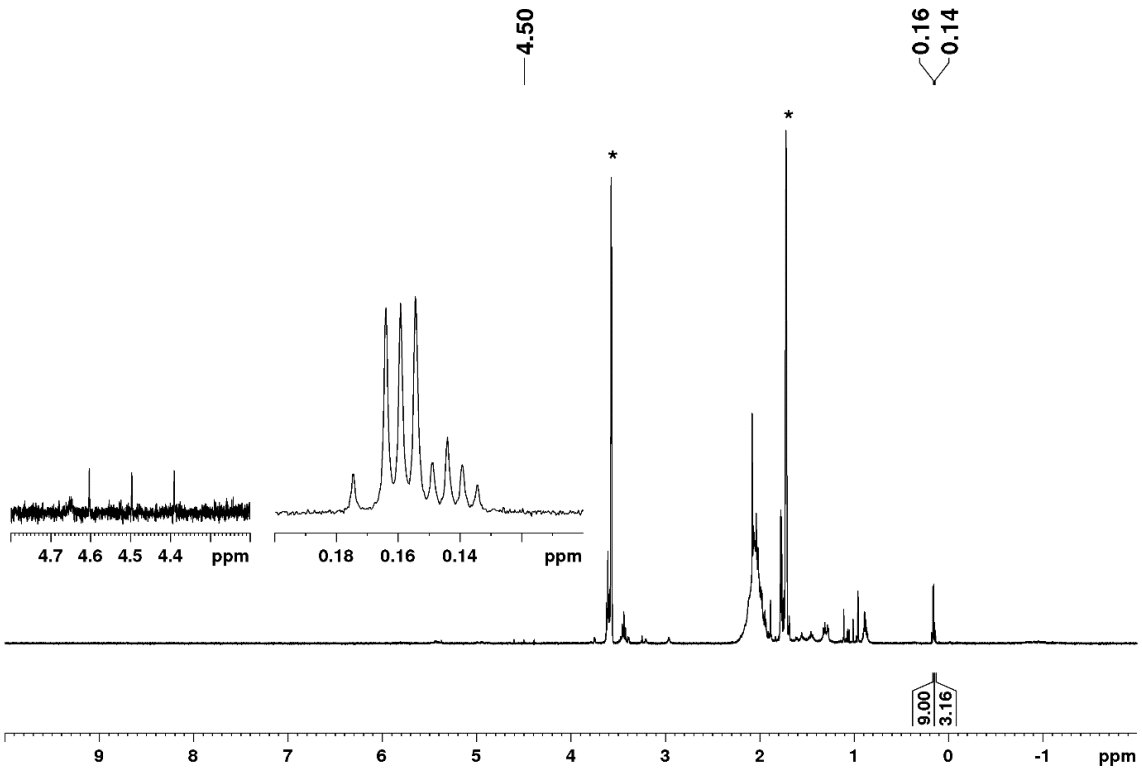

Figure S19. ^{1}H NMR spectrum (400 MHz) of $\mathbf{1}^{Y}$ in [D_8]THF at 26 °C, 5 minutes after addition of [D_4]methanol. The solvent residual signals are marked with an asterisk.

Crystallography

X-Ray Crystallography and Crystal Structure Determinations.

Single-crystals of $\mathbf{1}^{Y}$ and $\mathbf{1}^{Dy}$ were grown by aggregation from diluted THF solutions. Suitable crystals for X-ray structure analyses were selected inside a glovebox, coated with Parabar 10312, and fixed on a nylon/loop glass fiber. All X-ray data were collected on a Bruker APEX II DUO instrument equipped with an IμS microfocus sealed tube and QUAZAR optics for MoK_{α} (λ = 0.71073 Å) radiation. The data collection was determined using COSMO[5] employing ω-scans. Raw data were processed using APEX[6] and SAINT,[7] corrections for absorption effects were applied by using SADABS.[8] The structures were solved by direct methods and refined against all data by full-matrix least-squares methods on F^2 using SHELXTL[9] and SHELXLE.[10] All non-hydrogen atoms were refined anisotropic. Hydrogen atoms for the CH_2 group, the hydrido, and most of the hydrogen atoms of the CH_3 groups were found in the difference Fourier map. All graphics were generated employing CCDC Mercury 4.3.1.[11] Further details regarding the refinement and crystallographic data are listed in Table S1 and in the CIF files. CCDC depositions 2181381 and 2181382 contain all the supplementary crystallographic data for this paper. These data can be obtained free of charge from The Cambridge Crystallographic Data Centre via www.ccdc.cam.ac.uk/data_request/cif.

Table S1. Crystallographic data for compounds $\mathbf{1^{Y}}$ and $\mathbf{1^{Dy}}$

	$\mathbf{1^{Y}}$	$\mathbf{1^{Dy}}$
CCDC	2181381	2181382
Formula	$C_{46}H_{81}Y_3O_3$	$C_{46}H_{81}Dy_3O_3$
M_r [g/mol]	948.83	1169.60
Color/shape	plate/yellow	plate/colorless
Crystal dimensions [mm]	0.287 x 0.255 x 0.099	0.098 x 0.096 x 0.045
Crystal system	monoclinic	triclinic
Space group	$P2_1/n$	$P\bar{1}$
a [Å]	12.5260(9)	11.3103(7)
b [Å]	19.1070(14)	11.9001(7)
c [Å]	18.9963(14)	21.1333(12)
α [°]	90	97.942(2)
β [°]	92.1920(10)	91.931(2)
γ [°]	90	114.983(2)
V [Å³]	4543.1(6)	2540.1(3)
Z	4	2
T [K]	100(2)	100(2)
λ [Å]	0.71073	0.71073
ρ_{calcd} [g/cm³]	1.387	1.529
μ [mm^{-1}]	3.837	4.400
F (000)	1992	1158
θ range [°]	1.945 – 30.536	1.915 – 24.634
independent reflections	13876	8536
reflections collected (I > 2σ)	103801	51818
R1/*w*R2 (I > 2σ)	0.0343/0.0707	0.0332/0.0697
R1/*w*R2 (all data)	0.0592/0.0789	0.0491/0.0763
GOF	1.008	1.019

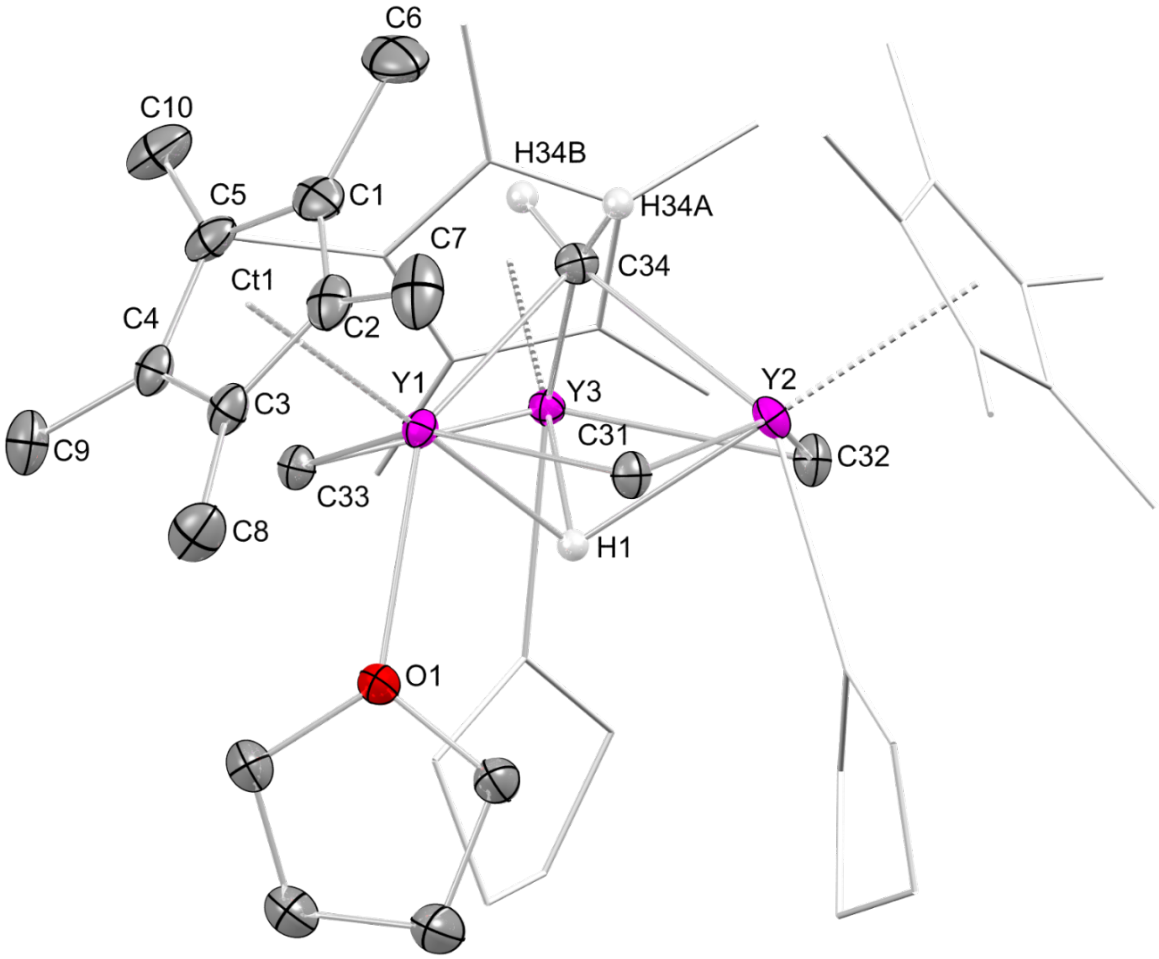

Figure S20. Crystal structure of $[Cp^*_3Y_3(\mu_2\text{-}CH_3)_3(\mu_3\text{-}CH_2)(\mu_3\text{-}H)(thf)_3]$ (**1**$^{\mathbf{Y}}$) with atomic displacement parameters set at the 50% probability level. Hydrogen atoms, except for methylidene hydrides and the μ_3-bridging hydride, are omitted for clarity. Ancillary Cp* ligands and coordinated THF (except for one each) are represented by a wireframe model for improved visualization. Selected interatomic distances [Å] and angles [°]: Y1–C1 2.705(2), Y1–C2 2.723(2), Y1–C3 2.782(2), Y1–C4 2.711(2), Y1–C5 2.700(2), Y1···Ct1 2.427, Y1–H1 2.22(2), Y2–H1 2.34(2), Y3–H1 2.29(2), Y1–C34 2.448(2), Y2–C34 2.422(2), Y3–C34 2.416(2), Y1–C31 2.572(2), Y1–C33 2.572(2), Y1–O1 2.4816(15), C34–H34A 0.921(19), C34–H34B 0.922(19), C1–C2 1.406(3), C2–C3 1.417(3), C3–C4 1.423(3), C4–C5 1.426(3), C5–C1 1.406(3), C1–C6 1.507(3), C1–C2–C3 108.2(2), C2–C3–C4 107.78(19), C3–C4–C5 107.42(19), C4–C5–C1 108.07(19), C5–C1–C2 108.5(2), Ct1···Y1–H1 178.62, Ct1···Y1–C31 104.87, Ct1···Y1–C33 105.24, Ct1···Y1–C34 111.46, Ct1···Y1–O1 105.69, Y1–C31–Y2 81.83(6), Y2–C32–Y3 81.01(6), Y1–C33–Y3 81.68(6), Y1–C34–Y2 87.74(7), Y1–C34–Y3 87.83(7), Y2–C34–Y3 87.08(7), Y1–H1–Y2 95.53, Y1–H1–Y3 96.71, Y2–H1–Y3 92.00, C31–Y1–H1 76.2(6), C33–Y1–H1 73.7(6), C34–Y1–H1 69.4(6), C34–Y1–O1 142.72(6), H1–Y1–O1 73.5(6).

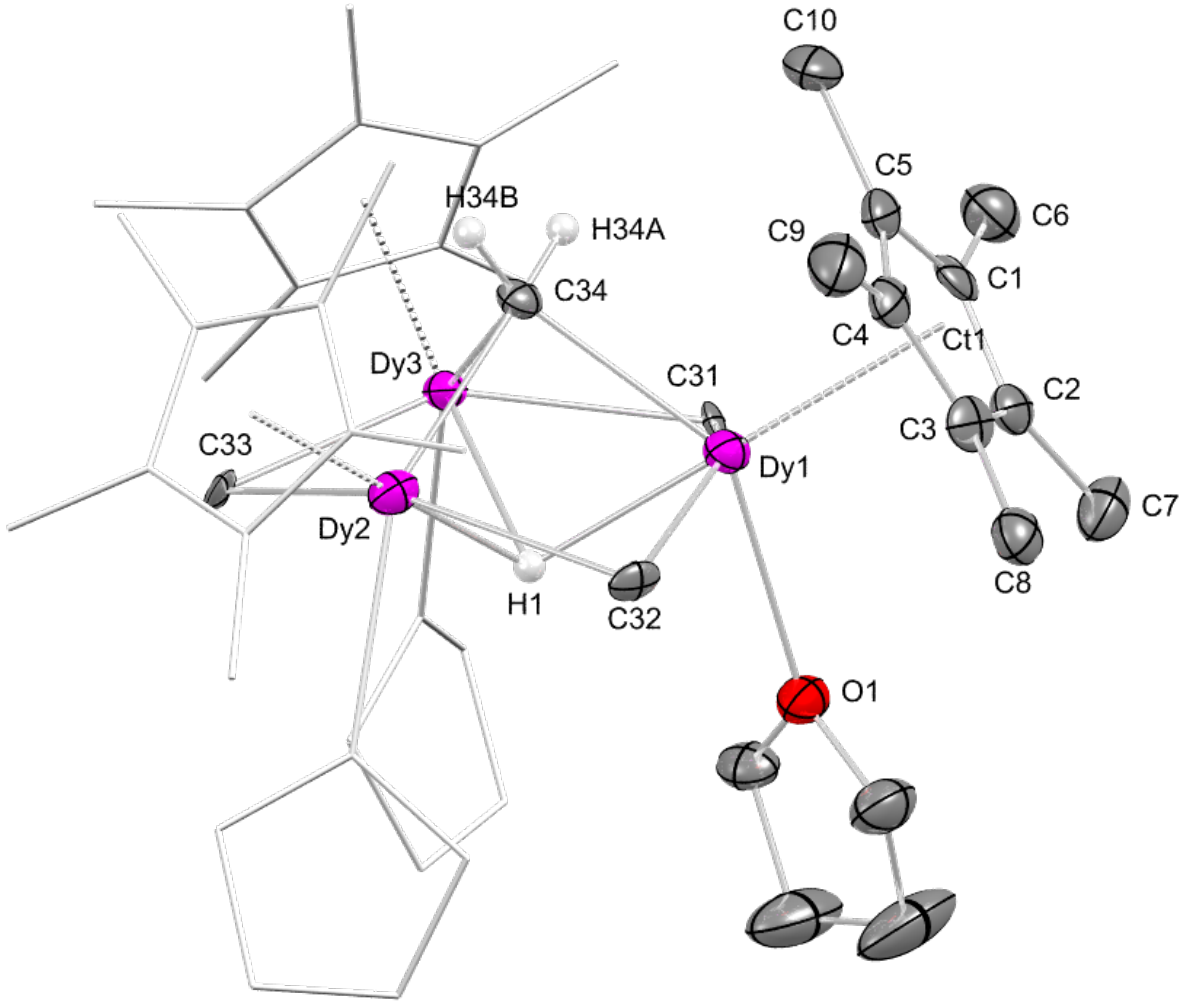

Figure S21. Crystal structure of $[Cp^*_3Dy_3(\mu_2\text{-}Me)_3(\mu_3\text{-}CH_2)(\mu_3\text{-}H)(thf)_3]$ (**1**^{Dy}) with atomic displacement parameters set at the 50% probability level. Hydrogen atoms, except for methylidene hydrides and the μ_3-bridging hydride, are omitted for clarity. Ancillary Cp* ligands and coordinated THF (except for one each) are represented by a wireframe model for improved visualization. Selected interatomic distances [Å] and angles [°]: Dy1–C1 2.733(6), Dy1–C2 2.707(6), Dy1–C3 2.694(5), Dy1–C4 2.716(6), Dy1–C5 2.731(6), Dy1···Ct1 2.436, Dy1–H1 2.26(6), Dy2–H1 2.31(5), Dy3–H1 2.29(5), Dy1–C34 2.420(6), Dy2–C34 2.384(6), Dy3–C34 2.445(6), Dy1–C31 2.584(5), Dy1–C32 2.568(6), Dy1–O1 2.532(4), C34–H34A 0.91(9), C34–H34B 1.02(8), C1–C2 1.421(8), C2–C3 1.419(9), C3–C4 1.416(8), C4–C5 1.398(9), C5–C1 1.402(9), C1–C6 1.494(9), C1–C2–C3 107.3(5), C2–C3–C4 108.1(5), C3–C4–C5 107.8(6), C4–C5–C1 108.9(5), C5–C1–C2 107.9(6), Ct1···Dy1–H1 177.82, Ct1···Dy1–C31 105.43, Ct1···Dy1–C32 106.30, Ct1···Dy1–C34 111.63, Ct1···Dy1–O1 106.73, Dy1–C32–Dy2 80.18(14), Dy2–C33–Dy3 80.52(16), Dy1–C31–Dy3 82.76(16), Dy1–C34–Dy2 87.97(19), Dy1–C34–Dy3 89.3(2), Dy2–C34–Dy3 87.63(19), Dy1–H1–Dy2 93.60, Dy1–H1–Dy3 97.47, Dy2–H1–Dy3 93.28, C31–Dy1–H1 72.4(14), C32–Dy1–H1 75.8(14), C34–Dy1–H1 68.6(14), C34–Dy1–O1 141.55(16), H1–Dy1–O1 73.0(14).

IR Spectroscopy

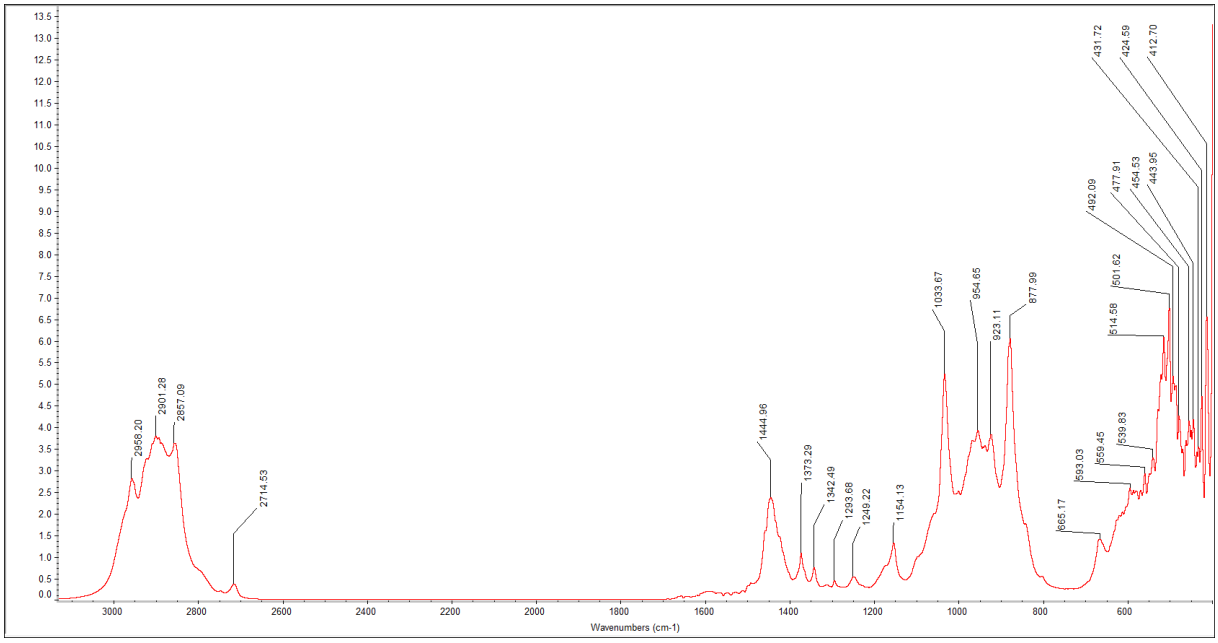

Figure S22. DRIFT spectrum of $[Cp^*_3Y_3(\mu_2\text{-}CH_3)_3(\mu_3\text{-}CH_2)(\mu_3\text{-}H)(thf)_3]$ ($\mathbf{1^Y}$).

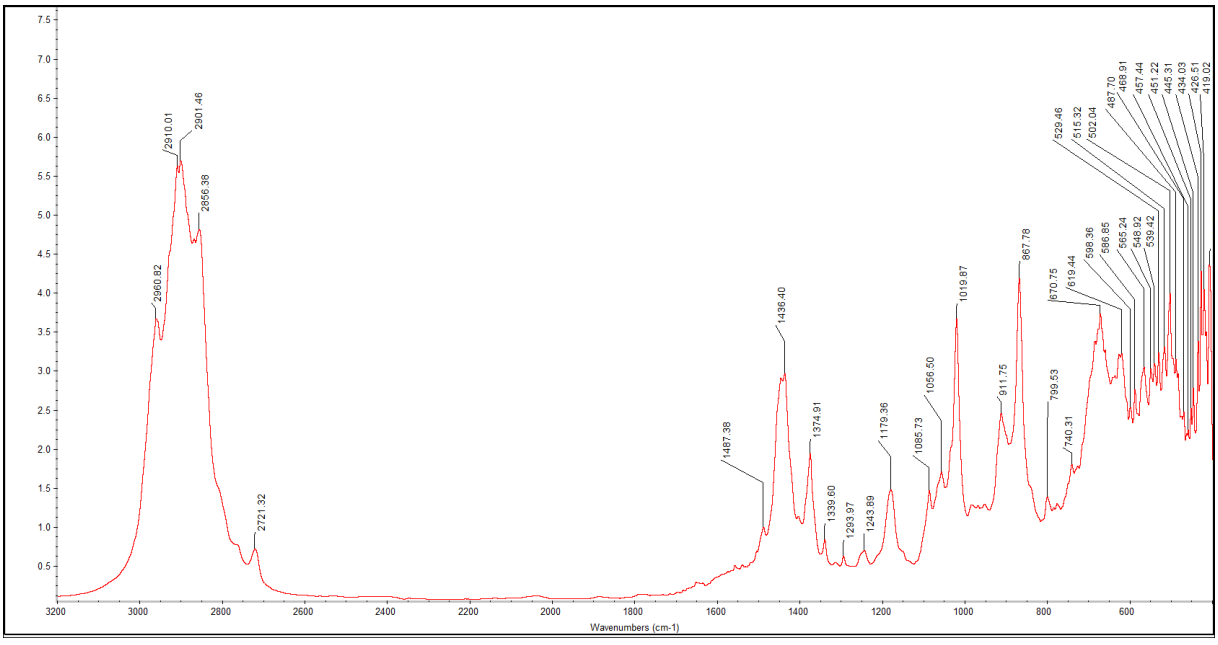

Figure S23. DRIFT spectrum of $[Cp^*_3Dy_3(\mu_2\text{-}CH_3)_3(\mu_3\text{-}CH_2)(\mu_3\text{-}H)(thf)_3]$ ($\mathbf{1^{Dy}}$).

References

1 G. Occhipinti, C. Meermann, H. M. Dietrich, R. Litlabø, F. Auras, K. W. Törnroos, C. c. Maichle-Mössmer, V. R. Jensen and R. Anwander, *J. Am. Chem. Soc.* 2011, **133**, 6323-6337.

2 H. M. Dietrich, K. W. Törnroos, E. Herdtweck and R. Anwander, *Organometallics* 2009, **28**, 6739-6749.

3 C. O. Hollfelder, M. Meermann-Zimmermann, G. Spiridopoulos, D. Werner, K. W. Törnroos, C. Maichle-Mössmer and R. Anwander, *Molecules* 2019, **24**, 3703.

4 C. O. Hollfelder, L. N. Jende, H. M. Dietrich, K. Eichele, C. Maichle-Mössmer and R. Anwander, *Chem. Eur. J.* 2019, **25**, 7298-7302.

5 COSMO, v. 1.61, Bruker AXS Inc., Madison, WI, 2012.

6 APEX 3, v. 2016.2015-2010; Bruker AXS Inc., Madison, WI, 2012.

7 SAINT, v. 8.34A; Bruker AXS Inc., Madison, WI, 2010.

8 L. Krause, R. Herbst-Irmer, G. M. Sheldrick and D. Stalke, *J. Appl. Crystallogr.* 2015, **48**, 3-10.

9 G. M. Sheldrick, *Acta Crystallogr. Sect. A* 2015, **71**, 3-8.

10 C. B. Hübschle, G. M. Sheldrick and B. Dittrich, *J. Appl. Crystallogr.* 2011, **44**, 1281-1284.

11 C. F. Macrae, P. R. Edgington, P. McCabe, E. Pidcock, G. P. Shields, R. Taylor, M. Towler and J. Streek, *J. Appl. Crystallogr.* 2006, **39**, 453-457.